Polyhedron 27 (2008) 3477–3483

Contents lists available at ScienceDirect

Polyhedron

journal homepage: www.elsevier.com/locate/poly

Syntheses, X-ray, MS^n, NMR and CD structure determination of nickel(II) complexes of Schiff bases of (*S*)-*N*-(2-benzoylphenyl)-1-benzylpyrrolidine-2-carboxamide and aromatic α-amino acids

Milan Nádvorník [a], Vratislav Langer [b], Robert Jirásko [c], Michal Holčapek [c], Tomáš Weidlich [d], Antonín Lyčka [e], Alexander Popkov [f,*]

[a] Department of General and Inorganic Chemistry, Faculty of Chemical Technology, University of Pardubice, nám. Čs. legií 565, 53210 Pardubice, Czech Republic
[b] Environmental Inorganic Chemistry, Department of Chemical and Biological Engineering, Chalmers University of Technology, SE-41296 Göteborg, Sweden
[c] Department of Analytical Chemistry, Faculty of Chemical Technology, University of Pardubice, nám. Čs. legií 565, 53210 Pardubice, Czech Republic
[d] Institute of Environment Protection, University of Pardubice, Doubravice 41, 533 41 Pardubice, Czech Republic
[e] Research Institute for Organic Syntheses, Rybitví 296, 532 18 Pardubice 20, Czech Republic
[f] Department of Nuclear Medicine and Molecular Imaging, University Medical Center Gronongen, University of Groningen, P.O. Box 30.001, 9700 RB Groningen, The Netherlands

ARTICLE INFO

Article history:
Received 2 April 2008
Accepted 8 August 2008
Available online 8 October 2008

Dedicated to Professor Yuri N. Belokon on the occasion of his 70th birthday

Keywords:
Nickel
Schiff base
α-Methyl amino acids
Chiral synthon
Protective groups
Circular dichroism

ABSTRACT

A preparative procedure for the synthesis of an important chiral synthon of side-chain protected tyrosine was developed and optimised for the minimisation of nickel salts waste. While preparing a similar side-chain protected tryptophan synthon, an unexpected low stability was found of the Boc-protective group of the tryptophan aromatic nitrogen during purification on silica gel. X-ray crystal structure determination, tandem mass spectrometry (MS/MS) and NMR were applied for the elucidation of the structures of the prepared complexes and by-products. Stereochemistry of products of α-methylation of the complexes was assessed using a model tyrosine-derived compound.

1. Introduction

Nickel(II) complexes of Schiff bases of (*S*)-*N*-(2-benzoylphenyl)-1-benzylpyrrolidine-2-carboxamide (BPB) and α-amino acids were developed as artificial analogues of pyridoxal 5′-phosphate (PLP)-dependent enzymes [1]. Their preparative applications for stoichiometric, asymmetric synthesis of α-amino acids are being perfected by a number of groups worldwide [2]. Significant steps have been made in reducing the environmental impact of the complexes' high-scale application. The most important feature is that BPB itself was initially designed as a reusable enzyme-like auxiliary [3]. In the synthesis of BPB no chromatographic steps are used [2f]. Recently, an improved synthesis of BPB was published in which work with the lacrymatory alkylating agent benzylchloride was avoided. In a catalytic process, less toxic benzaldehyde was used without any reduction of isolated product [4]. Preparation of the complexes from BPB, nickel nitrate, sodium methoxide and various α-amino acids results in the release of nickel to waste water. For the most frequently used complex derived from the simplest α-amino acid glycine, a modified procedure was developed [5]. It allowed for a significant decrease in the amount of nickel in waste water. The question arises as to whether it is possible to reduce the amount of nickel in waste water in the preparation of complexes derived from other proteinogenic α-amino acids. Such complexes are being prepared in lower amounts than the complex derived from glycine, but their consumption is increasing, *e.g.* for the preparation of *O*-(2′-[^{18}F]fluoroethyl)-L-tyrosine [6] and α-methyl amino acids for positron emission tomography (PET) [7] or other quaternary α-amino acids [8]. In this work, we investigated the dependence of the yields of the complexes derived from side-chain protected tyrosine or tryptophan on the amount of nickel nitrate and amino acid employed. Both amino acids' side chains were protected by *tert*-Bu- and Boc-protective groups, respectively (Scheme 1). Compatibility of these standard side-chain protective groups for Fmoc-strategy of peptide synthesis was assessed in relation to the reaction conditions used for the preparation of the complexes. Stereochemistry of products of α-methylation of the

* Corresponding author.
E-mail address: sasha@jcu.cz (A. Popkov).

0277-5387/$ - see front matter © 2008 Elsevier Ltd. All rights reserved.
doi:10.1016/j.poly.2008.08.009

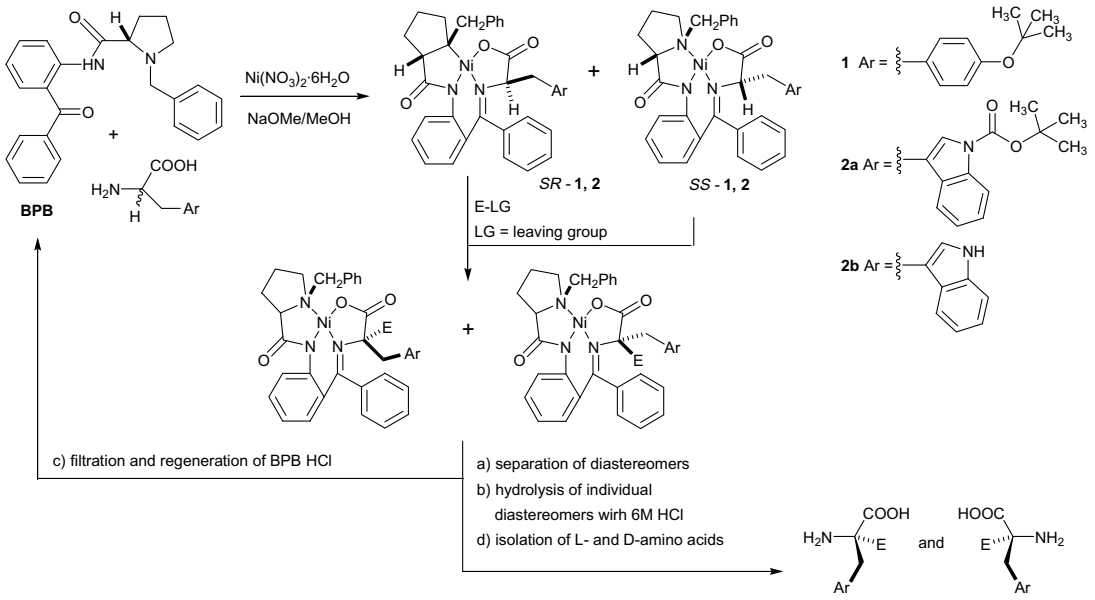

Scheme 1.

complexes was assessed using a model complex derived from tyrosine protected by a methyl group in the side chain.

2. Results and discussion

Ratios of starting compounds for the preparation of complexes were chosen from a previous optimisation protocol of the ratio of starting compounds for the preparation of the glycine-derived complex [5]. Twenty percent excess of nickel nitrate(II) to BPB was predicted to be optimal for both maximisation of the yield of complexes and minimisation of the amount of nickel in waste water. Five and fifty percent excess were also tested (Table 1). Unlike glycine used in the previous work, both side-chain protected amino acids are relatively expensive. Thus, the previously applied two-fold excess of amino acid was considered to be uneconomical. Ten, twenty and forty percent excess of amino acid to BPB were tested (Table 1). Experiments demonstrated that in this particular case the Boc-protective group of the indole residue nitrogen is unstable during chromatographic purification on silica gel. A significant amount of the complex derived from the protected tryptophan lost the protective group during quick preparative TLC purification of an analytical sample. Clean deprotection was observed in all the four preparative syntheses followed by time-consuming purification of the product by column chromatography on silica gel. No observations of low stability of indole nitrogen Boc-protected derivatives of tryptophan [9] were found in the literature. Deprotection was confirmed by NMR, MS/MS and X-ray data. In order to demonstrate the necessity of including the protective group for the preparation of quaternary α-amino acids via C-methylation of carbanion generated from tertiary precursor [7b], a sample of deprotected complex was methylated with an excess of CH_3I/KOH in 1,3-dimethylimidazolidin-2-one (DMI). This resulted in pure N-methylated product without any traces of the C-methylated product as confirmed by both MS^n and X-ray data (Scheme 2, Figs. 1C, D, 2 and 3).

Table 1
Yields of complexes (both *SS* and *SR* diastereomers) depending on the ratios of the starting compounds used

$Ni(NO_3)_2 \cdot 6H_2O$ excess	Amino acid excess	BPB	Yield of complex **1** (sum of diastereomers)	Yield of complex **2b** (sum of diastereomers)
1.05	1.1	1	57	55
1.2	1.2	1	79	61
1.2	1.4	1	83	86
1.5	1.4	1	87	79

Development of an alternative purification method was successful, but the methylation of the *N*-Boc protected complex with an excess of CH_3I/KOH in DMI resulted in complete deprotection followed by complete N-methylation [10]. Similar *N*-Si(*i*-Pr)$_3$ protected tryptophan complex is stable during chromatographic purification on silica gel, but its methylation with an excess of CH_3I/KOH in DMI also resulted in almost complete deprotection followed by predominant N-methylation and less than 1% of C-methylation (Scheme 3). *tert*-Butyl protection of the phenolic group of tyrosine is perfectly compatible with the reaction conditions used and with column chromatography on silica gel (Fig. 1A, B).

Typical ions in the first-order positive-ion ESI mass spectra are protonated molecules and adducts with alkali metal ions, such as $[M+Na]^+$ and $[M+K]^+$ (Fig. 1A). The presence of these ions was used for the determination of molecular weights of all analysed compounds (see Section 3 for more details). Based on the determination of the molecular weights, the presence or the absence of a protective group or another substituent on the aromatic nitrogen (for tryptophan) or oxygen atom (for tyrosine side-chains) can be recognised [10]. Furthermore, the presence of a protective group can be confirmed using tandem mass spectrometry by the typical neutral losses associated with a particular group. In the case of complex 1, the typical neutral losses are $\Delta m/z$ 56 (butene) and 106 (see Fig. 1B). For deprotected complex 2b, the characteristic neutral loss is $\Delta m/z$ 129 (see Fig. 1C). However, the difference neutral loss $\Delta m/z$ 145 is observed in the spectra of N-methylated complex 3 (see Fig. 1D).

Both complexes *SS*-**2b** and *SS*-**3** crystallize with solvent molecules in the crystalline lattice. The crystals loose some solvent molecules during drying in air at ambient temperature. For such crystallosolvates, X-ray crystallography of shock-frozen single crystals is an informative method of structure characterisation.

2.1. SS-*2b*

There are 2 crystallographically different complexes co-crystallized with 3 benzene molecules in the asymmetric unit. Both complexes suffer from disorder at C2 atoms and one of them even has

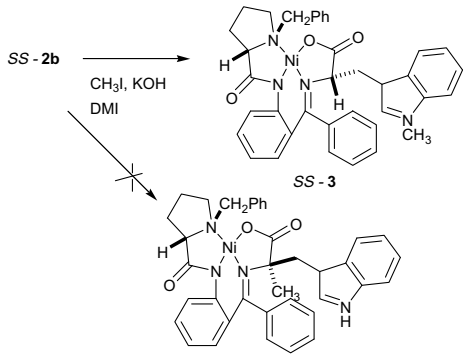

Scheme 2.

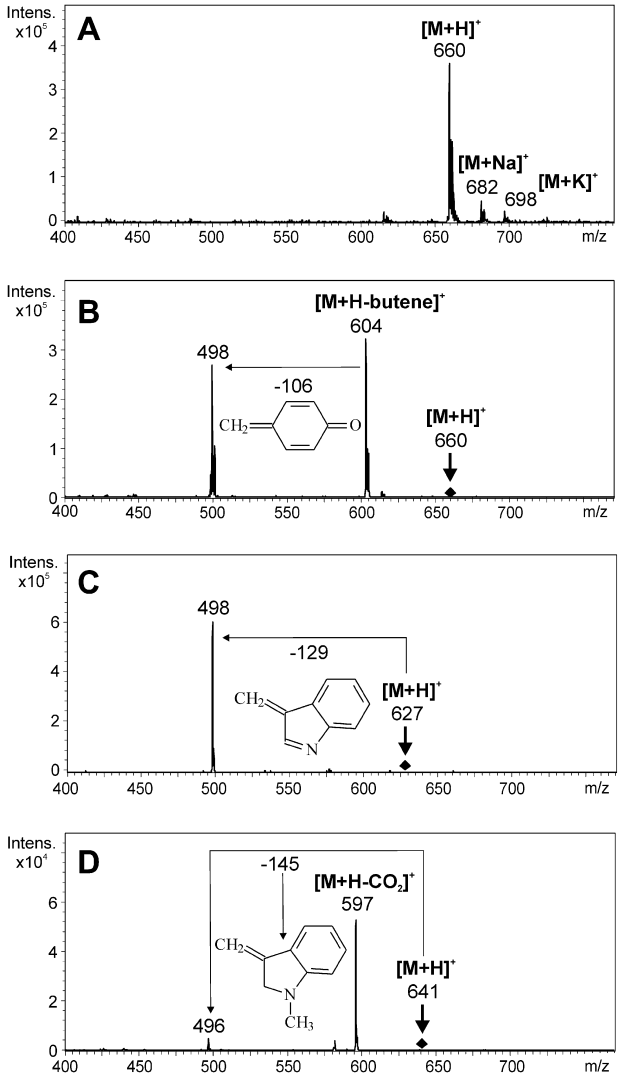

Fig. 1. Positive-ion electrospray ionization mass spectra: (A) First-order spectrum of **1**, (B) MS/MS spectrum of ion *m*/*z* 660 $[M+H]^+$ for **1**, (C) MS/MS spectrum of ion *m*/*z* 627 $[M+H]^+$ for **2b**, (D) MS/MS spectrum of ion *m*/*z* 641 $[M+H]^+$ for **3**.

the disorder of the phenyl group, see Figs. 2 and 5 (in Supplementary material). There are hydrogen bonds in the structure producing an helical arrangement of the complexes, see Figs. 6 and 7 (in Supplementary material). Packing in the unit cell along the monoclinic *b*-axis is shown in Fig. 8 (in Supplementary material).

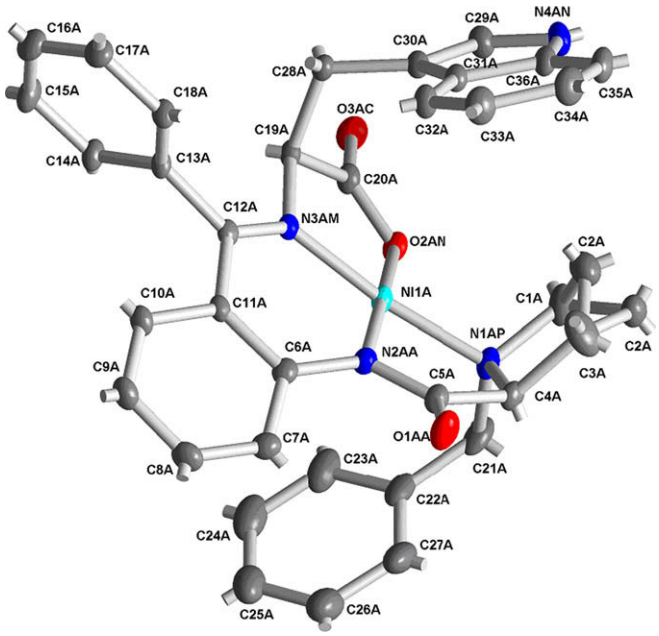

Fig. 2. The numbering scheme for *SS*-**2b**, the first complex, with atomic displacement ellipsoids at 30% probability level. Note disorder of C2A. Hydrogens are omitted for clarity.

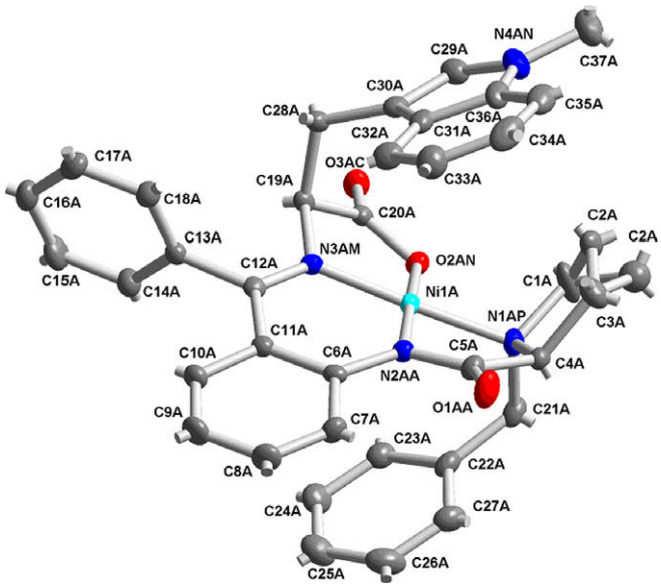

Fig. 3. The numbering scheme for *SS*-**3**, the first complex, with atomic displacement ellipsoids at 30% probability level. Note disorder of C2A. Hydrogens are omitted for clarity.

2.2. *SS*-**3**

There are 2 crystallographically different complexes co-crystallized with 2 benzene and 2 water molecules in the asymmetric unit. Again, both complexes suffer from disorder at C2 atoms see Figs. 3 and 9 (in Supplementary material). There are hydrogen bonds in the structure producing an helical arrangement of the complexes, see Figs. 10 and 11 (in Supplementary material). Packing in the unit cell along the orthorhombic *a*-axis is shown in Fig. 12 (in Supplementary material).

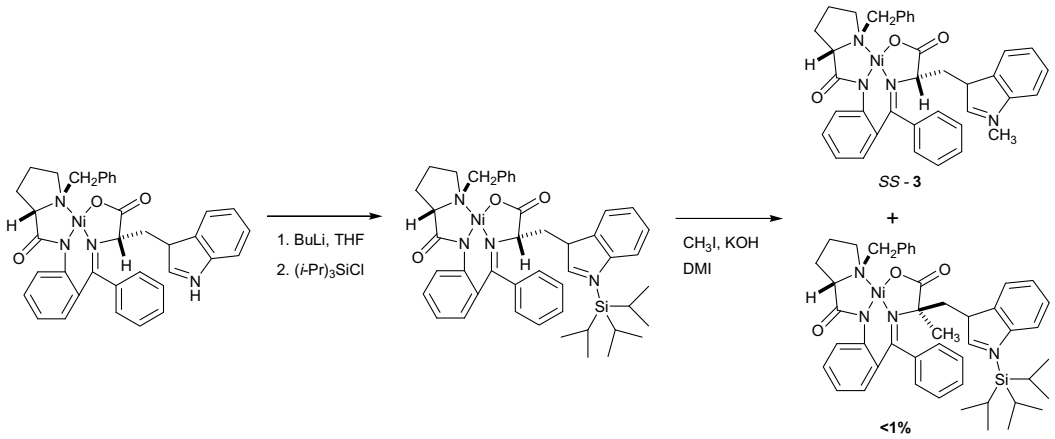

Scheme 3.

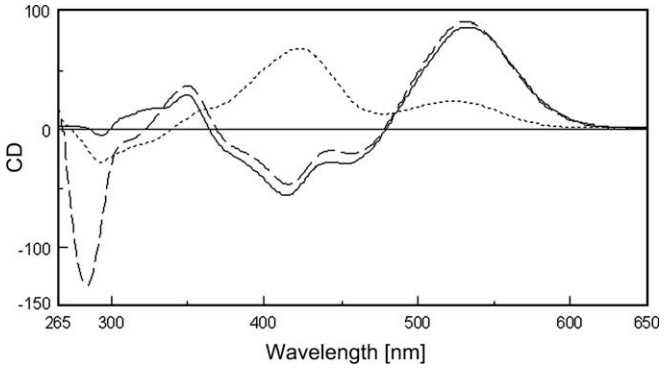

Fig. 4. CD spectra of *SS*-**4** (—), the first fraction, *SS*-**5** (— — —) and the second fraction *SR*-**5** (. . . . . .).

For both structures, the absolute structures were unambiguously determined. All nickel complexes show square-planar coordination geometry with small pyramidal distortions.

Five and ten percent excess of nickel nitrate and amino acid, respectively, led to poor yields of both complexes (Table 1). This result corresponds with the low yield of glycine-derived complex obtained with five percent excess of nickel nitrate [5]. As expected, twenty percent excess of nickel nitrate led to the high yield of both complexes. With such an excess of nickel salt, a higher excess of amino acid gave a slightly higher excess of complex **1** derived from tyrosine, and led to significantly higher yield of the complex derived from tryptophan (**2a** → **2b**) (Table 1). Lower yield of this complex, in the case when fifty percent excess of nickel nitrate was used, is consistent with the previously observed relationship between an excess of nickel nitrate used and yields of the complexes derived from glycine. Diastereomeric excess of (*SS*)-diastereomers in all cases was >95%. Minor (*SR*)-diastereomers were collected and partially characterised. Due to retroracemisation of the amino acid chiral centre in basic conditions, in further alkylation reaction mixtures of both diastereomers could be used without separation [8].

Due to poor preparative TLC separation of diastereomeric products of α-methylation of complex *SS*-**1**, its analogue complex *SS*-**4** (carrying methyl protective group of the side chain instead of *tert*-Bu) was used to assess the stereochemistry of products of α-methylation of such complexes (Scheme 4). These diastereomeric products of methylation *SS*-**5** and *SR*-**5** are separable by preparative TLC on silicagel while for the separation of many other similar diastereomers expensive preparative HPLC is necessary.

Stereochemistry of the diastereomers of 5 was assessed by circular dichroism (CD) and ^{13}C NMR spectroscopy:

- Two intense peaks were observed in the ^{13}C NMR spectrum of the reaction mixture after alkylation of *SS*-**4** with $^{13}CH_3I$/KOH in DMI (Scheme 4): minor at δ 29.3 ppm and major at δ 28.5 ppm. According to the integral intensities of peaks in ^{13}C NMR spectra, the diastereomeric excess of methylation was 6.9%;
- Two fractions were obtained after the preparative TLC separation of the reaction mixture. The first fraction giving a main ^{13}C NMR peak at δ 29.3 ppm was associated with the minor diastereomer. The second fraction where the main peak was at δ 28.5 ppm, was associated with the major diastereomer;
- CD spectra of starting *SS*-**4** and both diastereomers of **5** were recorded. Cotton effects in the spectra of both *SS*-**4** and the first TLC fraction (minor diastereomer) of **5** were similar in two areas (650–480 nm and 480–360 nm). Cotton effect in the spectrum of the second TLC fraction (major diastereomer) of **5** in the range 480–360 nm had an opposite sign (Fig. 4). Based on these CD data, the *SS* configuration was assigned to the first fraction (minor diastereomer) and the *SR* configuration was assigned to the second fraction (major diastereomer). This assignment is consistent with the proposed predominance of *Si*-alkylation leading to the major formation of *SR*-**5** (Scheme 4)[8].

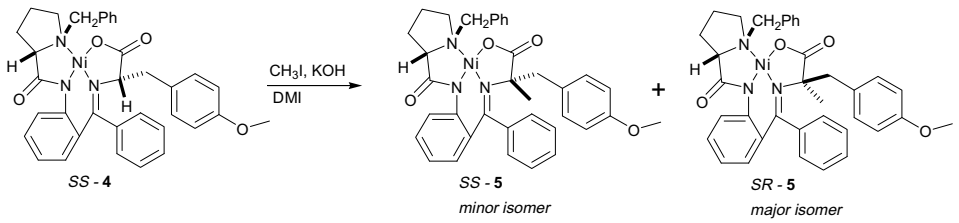

Scheme 4.

3. Experimental

The ^1H and ^{13}C NMR spectra were obtained in $CDCl_3$ solutions using a Bruker AMX-360 or Bruker 500 spectrometer equipped with a multinuclear 5 mm tunable probe. ^1H NMR chemical shifts δ are expressed in parts per million (ppm) downfield from tetramethylsilane as an internal standard. Coupling constants *J* are given in Hz. ^{13}C NMR chemical shifts are given with respect to the solvent signal (δ = 77 ppm). Data are given in the following order: δ value (number of protons, multiplicity (s, singlet; d, doublet; dd doublet of doublet; m, multiplet; t, triplet; br s, broad singlet).

Positive-ion electrospray ionization (ESI) mass spectra were measured on an Esquire 3000 ion trap analyzer (Bruker Daltonics, Bremen, Germany) in the range *m*/*z* 50–1000. The samples were dissolved in 100% acetonitrile and analyzed by direct infusion at the flow rate 5 μl/min. The selected precursor ions were further analyzed by MS/MS analyses under the following conditions: the isolation width *m*/*z* = 8, the collision amplitude (in the range 0.8–1.0 V depending on the precursor ion stability), the ion source temperature (300 °C), the tuning parameter compound stability (100%), the flow rate and the pressure of nitrogen (4 l/min and 10 psi), respectively. The elemental composition of the complexes *SS*-**1** and *SS*-**2b** was confirmed on an orthogonal hybrid quadrupole time-of-flight (QTOF) mass spectrometer fitted with electrospray ionization source (Bruker Daltonics). The instrument was externally calibrated using ESI tunning mix before the measurement. The samples were dissolved in acetonitrile and analyzed by direct infusion at the flow rate of 3 μl/min. Interface parameters were set as follows: capillary voltage −4.5 kV, drying temperature 200 °C, the flow rate and pressure of nitrogen were 4 l/min and 0.4 bar, respectively. For the recording of exact masses, QTOF data were acquired by the summation of 50 000 scans with 10 rolling averages. The typical ions observed in the first-order positive-ion mass spectra were $[M+H]^+$, $[M+Na]^+$ and $[M+K]^+$, and the elemental composition was confirmed by the comparison of experimental and theoretical values for all studied compounds. Table 2 shows mass accuracies for monoisotopic masses, mean mass accuracies correspond to the mean value for all isotopic peaks, and the sigma is a combined value for the standard deviation of masses and intensities for all peaks.

The elemental composition of the complexes *SS*-**5** and *SR*-**5** was confirmed on a sector mass spectrometer fitted with electron-impact ionization source (VG Analytical) by a commercial analytical laboratory.

Diffraction data were collected using a Siemens SMART CCD diffractometer with Mo Kα radiation (λ = 0.71073 Å, graphite monochromator). The crystals were cooled to 173(2) K by a flow of nitrogen gas using the LT-2A device. A full sphere of reciprocal space was scanned by 0.3 steps in ω with a crystal-to-detector distance of 3.97 cm. Preliminary orientation matrices were obtained from the first frames using SMART program. The collected frames were integrated using the preliminary orientation matrices which were updated every 100 frames. Final cell parameters were obtained by refinement of the positions of reflections with $I > 10\sigma(I)$ after the integration of all the frames using SAINT software [11]. The data were empirically corrected for absorption and other effects using the SADABS program [12]. The structures were solved by direct methods and refined by full-matrix least-squares analysis on all $|F^2|$ data using SHELXTL software [13]. The crystallographic and refinement data are summarized in Tables 3 and 4. The hydrogen bonding geometrical parameters are summarized in Tables 5 and 6 (in Supplementary material). Selected bond lengths, selected bond angles and their estimated standard deviations are listed in Tables 7 and 8 (in Supplementary material). The molecular graphics (Figs. 2,3,5–12) were prepared using the program DIAMOND [14]. Circular dichroism spectra were recorded using a Jasco J-715 spectropolarimeter.

Table 2
Mass accuracies and sigma values used

		$[M+H]^+$	$[M+Na]^+$	$[M+K]^+$
Complex *SS*-**1**	Mass accuracy (ppm)	1.0	0.3	0.7
$C_{38}H_{39}N_3O_4Ni$	Mean mass accuracy (ppm)	−1.4	−0.3	0.6
	Sigma	0.015	0.005	0.025
Complex *SS*-**2b**	Mass accuracy (ppm)	1.5	0.6	0.0
$C_{36}H_{32}N_4O_3Ni$	Mean mass accuracy (ppm)	−0.7	0.548	0.0
	Sigma	0.025	0.013	0.024

3.1. General procedure for the synthesis of complexes

2.47 M MeONa/MeOH (7.9 ml, 19.5 mmol) was added to a stirred suspension of BPB (500 mg, 1.3 mmol) and the corresponding amount of nickel nitrate and protected amino acid (Table 1) in dry MeOH (4 ml) under argon at 50 °C. The volume of the reaction mixture was then adjusted to 20 ml with dry MeOH. After stirring at 55 °C for 30 min, the mixture was poured into 0.7% aqueous citric acid (300 ml), stirred and the resulting precipitate was filtered off, washed with water on a filter and dried on air. The dry precipitate was purified by column chromatography using silica gel (Merck 40/63) and eluted with chloroform.[1] The first red fractions containing minor (*SR*)-diastereomers and the second red fractions containing major (*SS*)-diastereomers were collected. Yields of complex formation are given in Table 1. Complexes *SS*-**2b** and *SS*-**3** were purified by preparative TLC followed by crystallisation from a (wet) acetone-benzene mixture which gave a crystallosolvate. Resulting red single crystals are unstable in air at ambient temperature; they loose benzene (and water in the case of *SS*-**3**) and decompose within tens of minutes.

3.1.1. (SR)-Diastereomer of complex **2b**

δ_H (360.13 MHz, $CDCl_3$; Me_4Si) 1.36 (2H, m), 1.84 (1H, m), 2.21 (1H, m), 2.30 (1H, m), 3.07 (5H, m), 3.64 (1H, m), 4.30 (1H, t), 6.76 (1H, m), 6.84 (1H, m), 7.05 (1H, m), 7.10 (3H, m), 7.15 (1H, m), 7.20 (1H, m), 7.31 (4H, m), 7.38 (2H, d), 7.49 (2H, m), 7.55 (2H, m), 8.39 (1H, br s, NH), 8.52 (1H, d). δ_C (90.57 MHz, $CDCl_3$) 23.57 CH_2, 30.92 CH_2, 31.11 CH_2, 54.91 CH_2, 58.66 CH_2, 68.30 CH, 72.25 CH, 110.35 C_q, 111.17 CH, 120.11 CH, 120.44 CH, 120.67 CH, 122.50 CH, 123.76 CH, 124.81 CH, 126.08 C_q, 127.19 CH, 128.16 CH, 128.55 2 × CH, 128.67 CH, 128.72 C_q, 128.81 CH, 129.27 CH, 129.69 CH, 131.76 C_q, 131.90 2 × CH, 132.59 CH, 133.76 CH, 134.83 C_q, 136.57 C_q, 143.23 C_q, 170.96 C_q, 179.22 C_q, 181.88 C_q.

3.1.2. (SS)-Diastereomer of complex **2b**

δ_H (360.13 MHz, $CDCl_3$; Me_4Si) 1.42 (1H, m), 1.79 (2H, m), 1.89 (1H, m), 2.11 (1H, m), 2.80 (1H, m), 3.07 (1H, dd, A part of AMX system), 3.21 (1H, dd, M part of AMX system), 3.36 (1H, dd, X part of AMX system), 3.40 (1H, d, A part of AB system of CH_2Ar, $^2J_{AB}$ 12.6), 4.21 (1H, d, B part of AB system of CH_2Ar, $^2J_{AB}$ 12.6), 4.35 (1H, t), 6.74 (2H, m), 6.92 (2H, m), 7.01 (1H, t), 7.19 (3H, m), 7.36 (6H, m), 7.56 (2H, m), 8.01 (2H, d), 8.30 (1H, d), 8.93 (1H, br s, NH). δ_C (90.57 MHz, $CDCl_3$) 22.58 CH_2, 30.22 CH_2, 30.52 CH_2, 56.91 CH_2, 63.12 CH_2, 70.27 CH, 71.55 CH, 109.41 C_q, 111.25 CH, 119.50 CH, 119.78 CH, 120.48 CH, 122.10 CH, 123.35 CH, 124.42 CH, 126.12 C_q, 127.17 CH, 127.90 CH, 128.26 Cq, 128.63 2 × CH, 128.65 CH, 128.70 CH, 128.95 CH, 129.58 CH, 131.42 2 × CH, 132.20 CH, 133.16 C_q, 133.45 CH, 134.03 C_q, 136.50 C_q, 142.68 C_q, 170.73 C_q,

[1] As chloroform is known to be a human carcinogen, for preparative applications a gradient elution using $CH_2Cl_2 \rightarrow CH_2Cl_2$: Me_2CO = 7:1 or toluene → toluene: Me_2CO = 2:1 is strongly recommended.

Table 3
Crystal data and structure refinement for *SS*-**2b**

Empirical formula	$C_{45}H_{41}N_4NiO_3$
Formula weight	744.53
Temperature (K)	173(2)
Wavelength (Å)	0.71073
Crystal system	monoclinic
Space group	$P2_1$
Unit cell dimensions	
a (Å)	15.5711(5)
b (Å)	9.6236(3)
c (Å)	25.6788(9)
α (°)	90
β (°)	106.729(1)
γ (°)	90
V (Å^3)	3685.1(2)
Z	4
D_{calc} (Mg/m^3)	1.342
Absorption coefficient (mm^{-1})	0.574
F(000)	1564
Crystal size (mm^3)	0.91 × 0.62 × 0.36
Theta range for data collection (°)	2.27–30.56
Index ranges	$-22 \leqslant h \leqslant 22$
	$-13 \leqslant k \leqslant 13$
	$-36 \leqslant l \leqslant 36$
Reflections collected	62093
Independent reflections	22451
	[R(int) = 0.0445]
Completeness to theta = 30.56°	99.7 %
Absorption correction	multi-scan
Maximum and minimum transmission	0.8200 and 0.6231
Refinement method	full-matrix least-squares on F^2
Data/restraints/parameters	22451/685/1030
Goodness-of-fit on F^2	1.055
Final R indices [I > 2sigma(I)]	R_1 = 0.0570
	wR_2 = 0.1428
R indices (all data)	R_1 = 0.0718
	wR_2 = 0.1519
Absolute structure parameter	0.019(9)
Largest difference in peak and hole (e Å^{-3})	1.392 and −0.445

Table 4
Crystal data and structure refinement for *SS*-**3**

Empirical formula	$C_{43}H_{42}N_4NiO_4$
Formula weight	737.52
Temperature	173(2) K
Wavelength	0.71073 Å
Space group	$P2_12_12_1$
Unit cell dimensions	
a (Å)	13.9338(2)
b (Å)	14.6081(2)
c (Å)	36.1605(5)
α (°)	90
β (°)	90
γ (°)	90
V (Å^3)	7360.34(18)
Z	8
D_{calc} (Mg/m^3)	1.331
Absorption coefficient (mm^{-1})	0.576
F(000)	3104
Crystal size (mm^3)	0.44 × 0.26 × 0.19
Theta range for data collection	2.10–25.00°
Index ranges	$-16 \leqslant h \leqslant 16$
	$-17 \leqslant k \leqslant 17$
	$-43 \leqslant l \leqslant 43$
Reflections collected	77400
Independent reflections	12942
	[R(int) = 0.0583]
Completeness to theta = 25.00°	99.8%
Absorption correction	multi-scan
Maximum and minimum transmission	0.8984 and 0.7857
Refinement method	Full-matrix least-squares on F^2
Data/restraints/parameters	12942/6/972
Goodness-of-fit on F^2	1.026
Final R indices [I > 2sigma(I)]	R_1 = 0.0518
	wR_2 = 0.1268
R indices (all data)	R_1 = 0.0593
	wR_2 = 0.1320
Absolute structure parameter	0.025(13)
Largest difference peak and hole (e Å^{-3})	1.141 and −0.378

179.47 C_q, 180.08 C_q. Positive-ion mass spectra: m/z 665 [M+K]$^+$, m/z 649 [M+Na]$^+$, m/z 627 ([M+H]$^+$, 100%), m/z 498 [M+H-129]$^+$. MS/MS of m/z 627: m/z 498 [M+H-129]$^+$. For the single crystal structure, see Fig. 2.

3.1.3. (SS)-Diastereomer of complex **3**

Positive-ion mass spectra: m/z 679 [M+K]$^+$, m/z 663 ([M+Na]$^+$, 100%), m/z 641 [M+H]$^+$. MS/MS of m/z 641: m/z 597 [M+H-CO2]$^+$, m/z 496 [M+H-145]$^+$. For the single crystal structure, see Fig. 3.

3.1.4. (SR)-Diastereomer of complex **1**

δ_H (360.13 MHz, $CDCl_3$; Me_4Si) 1.34 (9H, s), 1.80 (1H, m), 1.99 (1H, m), 2.38 (1H, m), 2.49 (1H, m), 2.60 (1H, m), 2.89 (1H, dd, A part of AMX system), 3.13 (2H, m, M part of AMX system and one of proline protons), 3.32 (1H, dd, X part of AMX system), 3.45 (1H, d, A part of AB system of CH_2Ar, $^2J_{AB}$ 12.7), 4.22 (1H, t), 4.28 (1H, d, B part of AB system of CH_2Ar, d, 1H, $^2J_{AB}$ 12.7), 6.65 (2H, m), 6.70 (1H, m), 6.97 (2H, m), 7.03 (2H, m), 7.16 (2H, m), 7.26 (1H, m), 7.31 (2H, t), 7.38 (1H, m), 7.51 (2H, m), 8.03 (2H, d), 8.23 (1H, d). δ_D (90.57 MHz, $CDCl_3$) 23.23 CH_2, 28.84 3 × CH_3, 30.80 CH_2, 39.54 CH_2, 57.32 CH_2, 63.22 CH_2, 70.39 CH, 71.66 CH, 78.28 C_q, 120.55 CH, 123.34 CH, 123.93 2 × CH, 126.12 C_q, 127.16 CH, 127.84 CH, 128.74 2 × CH, 128.76 CH, 128.80 CH, 128.95 CH, 129.64 CH, 130.10 C_q, 130.95 2 × CH, 131.49 2 × CH, 132.28 CH, 133.25 C_q, 133.49 CH, 134.09 C_q, 142.77 C_q, 155.21 C_q, 171.00 C_q, 178.62 C_q, 180.44 C_q.

3.1.5. (SS)-Diastereomer of complex **1**

δ_H (360.13 MHz, $CDCl_3$; Me_4Si) 1.28 (1H, m), 1.33 (9H, s), 1.53 (1H, m), 1.94 (1H, m), 2.14 (1H, m), 2.68 (1H, m), 2.85 (1H, dd, A part of AMX system), 2.98 (1H, dd, M part of AMX system), 3.48 (1H, d, A part of AB system of CH_2Ar $^2J_{AB}$ 13.8), 3.54 (1H, dd, X part of AMX system), 3.74 (1H, d, B part of AB system of CH_2Ar $^2J_{AB}$ 13.8Hz), 4.05 (1H, m), 4.20 (1H, t), 6.77 (2H, m), 6.96 (1H, d), 7.07 (2H, m), 7.17 (2H, m), 7.30 (1H, m), 7.38 (3H, m), 7.51 (6H, m), 8.43 (1H, d). δ_C (90.57 MHz, $CDCl_3$) 23.60 CH_2, 28.81 3 × CH_3, 31.19 CH_2, 39.41 CH_2, 56.50 CH_2, 60.59 CH_2, 69.14 CH, 71.72 CH, 78.44 C_q, 120.81 CH, 123.80 CH, 124.12 2 × CH, 126.36 C_q, 127.19 CH, 127.89 CH, 128.68 2 × CH, 128.78 CH, 128.81 CH, 129.23 CH, 129.79 CH, 130.39 C_q, 131.54 2 × CH, 132.08 2 × CH, 132.51 C_q, 132.58 CH, 133.73 CH, 134.16 C_q, 143.08 C_q, 155.29 C_q, 171.01 C_q, 178.42 C_q, 181.74 C_q. Positive-ion mass spectra: m/z 698 [M+K]$^+$, m/z 682 [M+Na]$^+$, m/z 660 ([M+H]$^+$, 100%). MS/MS of m/z 660: m/z 604 [M+H-butene]$^+$, m/z 498 [M+H-butene-106]$^+$.

(*SS*)-diastereomer of complex **4** was prepared according to the published procedure [15].

3.1.6. α-(*^{13}C*)Methylation of SS-4

Under an atmosphere of Ar at 20 °C to a solution of *SS*-**4** (62 mg, 0.1 mmol) in DMI (3 ml), excess of KOH and $^{13}CH_3I$ (63 μl, 1 mmol) was added and the reaction mixture was stirred for 30 min. The reaction mixture was poured into 10% aqueous citric acid (50 ml), stirred and the resulting red oil was filtered off. The filter was dried and extracted with chloroform. The extract was evaporated in vacuo. The diastereomeric excess was calculated based on the ratio of the integral intensities of the $^{13}CH_3$-signals in the ^{13}C NMR spectra of the mixtures of the diastereomers. *SS*-**5** and *SR*-**5** were separated by preparative TLC using silica gel (Merck 60H) eluted with CH_2Cl_2. Yield of *SS*-**5** and *SR*-**5** varies (40–70%) depending on the dryness of KOH used for the synthesis.

*3.1.7. (SS)-Diastereomer of complex **5***

The first fraction, red solidified oil, *SS*-**5**. The obtained complex was then purified by chromatography on Sephadex LH-20 with toluene: MeOH = 2:1. δ_H (500.13 MHz, $CDCl_3$; Me_4Si) 8.10 (1H, d), 7.99 (2H, m), 7.47 (1H, m), 7.37 (1H, m), 7.30 (5H, m) 7.25 (1H, s), 7.20 (1H, m), 7.10 (2H, m), 6.98 (3H, m), 6.59 (2H, s), 4.29 (1H, d, A part of AB system of CH_2Ar, $^2J_{AB}$ 12.6 Hz) and 3.54 (1H, d, B part of AB system of CH_2Ar, $^2J_{AB}$ 12.6 Hz), 3.81 (3H, s), 3.27 (1H, m), 3.10 (2H, m), 2.34 (1H, m), 2.24 (2H, m), 2.10 (1H, m), 1.91 (1H, m), 1.70 (1H, m), 1.13 (3H, $^{13}CH_3$, d, ^1J(H, C) = 130 Hz). δ_C (125.77 MHz, $CDCl_3$) 29.32 ($^{13}CH_3$). Calculated mass for $C_{35}{}^{13}CH_{35}N_3O_4Ni$ $[M]^+$ = 632.2015. High resolution EI-MS found $[M]^+$ = 632.2015.

*3.1.8. (SR)-Diastereomer of complex **5***

The second fraction, red crystals, *SR*-**5**. The obtained complex was then purified by chromatography on Sephadex LH-20 with toluene: MeOH = 2:1. Mp 274–276 °C (from acetone). δ_H (500.13 MHz, $CDCl_3$; Me_4Si) 7.86 (1H, d), 7.75 (2H, m), 7.51 (1H, m), 7.41 (2H, m), 7.33 (2H, m), 7.25–7.01 (6H, m), 6.94 (2H, m), 6.70 (1H, m), 6.62 (1H, t), 4.13 (1H, d, A part of AB system of CH_2Ph, $^2J_{AB}$ 14.3 Hz) and 3.39 (1H, d, B part of AB system of CH_2Ph, $^2J_{AB}$ 14.3 Hz), 3.72 (3H, s), 3.32 (1H, m), 3.06 (1H, m), 2.99 (1H, d, A part of AB system of CH_2Ar, $^2J_{AB}$ 14.7 Hz) and 2.86 (1H, d, B part of AB system of CH_2Ar, $^2J_{AB}$ 14.7 Hz), 2.32 (1H, m), 2.13 (2H, m), 1.91 (1H, m), 1.42 (3H, $^{13}CH_3$, d, ^1J(H, C) = 130 Hz).). δ_C (125.77 MHz, $CDCl_3$) 28.58 ($^{13}CH_3$). Calculated mass for $C_{35}{}^{13}CH_{35}N_3O_4Ni$ $[M]^+$ = 632.2015. High resolution EI-MS found $[M]^+$ = 632.2018.

NMR data are consistent with published data for similar complexes derived from α-methylphenylalanine or α-methyltyrosine-(OBn) [8a]. Half-minute intervals between pulses were applied for the recording of integral intensities of signals in ^{13}C NMR spectra.

4. Conclusions

A preparative procedure for the synthesis of a practically important chiral synthon of side-chain protected tyrosine was developed and optimised for the maximum reduction of nickel salts waste. While preparing a similar side-chain protected tryptophan synthon, unexpected low stability of Boc-protective group of tryptophan aromatic nitrogen was found during purification on silica gel. Stereochemistry of diastereomers of α-methylated complexes was disclosed using model compounds.

Acknowledgements

The authors thank Mr. Joe Bird and Dr. Katrin Probst for language corrections and acknowledge the support of Project Grants MSM0021627501 and MSM0021627502 sponsored by the Ministry of Education, Youth and Sports of the Czech Republic.

Appendix A. Supplementary data

Supplementary data associated with this article can be found, in the online version, at doi:10.1016/j.poly.2008.08.009.

References

[1] H.C. Dunathan, Adv. Enyzmol. Relat. Areas Mol. Biol. (1971) 79.
[2] (a) Y.N. Belokon, Izv. Acad. Nauk, Ser. Khim. (1992) 1106;
(b) Y.N. Belokon, Bull. Russ. Acad. Sci., Div. Chem. Sci. 41 (1992) 868 (Engl. Trans.) and references cited therein;
(c) Y.N. Belokon, Pure Appl. Chem. 64 (1992) 191;
(d) V.A. Soloshonok, D.V. Avilov, V.P. Kukhar, V.I. Tararov, T.F. Saveleva, T.D. Churkina, N.S. Ikonnikov, K.A. Kochetkov, S.A. Orlova, A.P. Pisarevsky, Y.T. Struchkov, N.I. Raevsky, Y.N. Belokon, Tetrahedron: Asymmetry 6 (1995) 1741;
(e) B.B. De, N.R. Thomas, Tetrahedron: Asymmetry 8 (1997) 2687;
(f) Y.N. Belokon, V.I. Tararov, V.I. Maleev, T.F. Saveleva, M.G. Ryzhov, Tetrahedron: Asymmetry 9 (1998) 4249;
(g) S. Collet, P. Bauchat, D. Danion-Bougot, R. Danion, Tetrahedron: Asymmetry 9 (1998) 2121;
(h) V.A. Soloshonok, C.Z. Cai, V.J. Hruby, Tetrahedron 55 (1999) 12045;
(i) X. Tang, V.A. Soloshonok, V.J. Hruby, Tetrahedron: Asymmetry 11 (2000) 2917;
(j) C. Cai, V.A. Soloshonok, V.J. Hruby, J. Org. Chem. 66 (2001) 1339;
(k) Y.N. Belokon, K.A. Kochetkov, N.S. Ikonnikov, T.V. Strelkova, S.R. Harutyunyan, A.S. Saghiyan, Tetrahedron: Asymmetry 12 (2001) 481;
(l) A. Debache, S. Collet, P. Bauchat, D. Danion, L. Euzenat, A. Hercouet, B. Carboni, Tetrahedron: Asymmetry 12 (2001) 761;
(m) A. Popkov, A. Gee, M. Nádvorník, A. Lyčka, Transition Met. Chem. 27 (2002) 884;
(n) O.V. Larionov, T.F. Saveleva, K.A. Kochetkov, N.S. Ikonnokov, S.I. Kozhushkov, D.S. Yufit, J.A.K. Howard, V.N. Khrustalev, Y.N. Belokon, A. de Meijere, Eur. J. Org. Chem. (2003) 869;
(o) Y.N. Belokon, K.A. Kochetkov, D.A. Borkin, Mendeleev Commun. (2003) 132;
(p) H. Ueki, T.K. Ellis, C.H. Martin, T.U. Boettiger, S.B. Bolene, V.A. Soloshonok, J. Org. Chem. 68 (2003) 7104;
(q) A.S. Saghiyan, A.V. Geolchanyan, S.G. Petrosyan, T.V. Ghochikyan, V.S. Haroutunyan, A.A. Avetisyan, Y.N. Belokon, K. Fischer, Tetrahedron: Asymmetry 15 (2004) 705;
(r) X.Y. Gu, J.A. Ndungu, W. Qiu, J.F. Ying, M.D. Carducci, H. Wooden, V.J. Hruby, Tetrahedron 60 (2004) 8233;
(s) S. Vadon-Legoff, S. Dijols, D. Mansky, J.-L. Boucher, Org. Process Res. Develop. 9 (2005) 677;
(t) V.A. Soloshonok, C. Cai, T. Yamada, H. Ueki, Y. Ohfune, V.J. Hruby, J. Am. Chem. Soc. 127 (2005) 15296;
(u) J.C. Pessoa, I. Correia, A. Galvão, A. Gameiro, V. Felix, E. Fiuza, J. Chem. Soc., Dalton Trans. (2005) 2312;
(v) A. Popkov, I. Císařová, J. Sopková, J. Jirman, A. Lyčka, K.A. Kochetkov, Collect. Czech. Chem. Commun. 70 (2005) 1397;
(w) A.S. Saghiyan, H.H. Hambardzumyan, L.L. Manasyan, A.A. Petrosyan, V.I. Maleev, A.S. Peregudov, Synth. Commun. 35 (2005) 449;
(x) A.S. Saghiyan, S.A. Dadayan, S.G. Petrosyan, L.L. Manasyan, A.V. Geolchanyan, S.M. Djamgaryan, S.A. Andreasyan, V.I. Maleev, V.N. Khrustalev, Tetrahedron: Asymmetry 17 (2006) 455;
(y) T. Kitamoto, S. Marubayashi, T. Yamazaki, Tetrahedron 64 (2008) 1888;
(z) Application of the complexes for preparation of helically chiral precursors of nanostructures:V.A. Soloshonok, H. Ueki, J. Am. Chem. Soc. 129 (2007) 2426.
[3] Y.N. Belokon, DSc. Thesis, A. N. Nesmeyanov Institute of Organoelement Compounds, Acad. Sci. USSR, 1979.
[4] V.I. Tararov, R. Kadyrov, C. Fischer, A. Börner, Synlett (2004) 1961.
[5] M. Nádvorník, A. Popkov, Green Chem. 4 (2002) 78.
[6] R.N. Krasikova, O.F. Kuznetsova, O.S. Fedorova, V.I. Maleev, T.F. Saveleva, Y.N. Belokon, Bioorg. Med. Chem. 16 (2008) 4994.
[7] (a) A. Popkov, M. Nádvorník, P. Kružberská, A. Lyčka, M. Eisenhut, N.M. Gillings, J. Labelled Compd. Radiopharm. 46 (2003) S227;
(b) A. Popkov, M. Nádvorník, P. Kružberská, A. Lyčka, S. Lehel, N.M. Gillings, J. Labelled Compd. Radiopharm. 50 (2007) 370;
(c) Y. Sakai, C. Dobson, M. Diksic, M. Aubé, E. Hamel, Neurology 70 (2008) 431;
(d) M.S. Judenhofer, H.F. Wehrl, D.F. Newport, C. Catana, S.B. Siegel, M. Becker, A. Thielscher, M. Kneilling, M.P. Lichy, M. Eichner, K. Klingel, G. Reischl, S. Widmaier, M. Röcken, R.E. Nutt, H.-J. Machulla, K. Uludag, S.R. Cherry, C.D. Claussen, B.J. Pichler, Nature Med. 14 (2008) 459;
(e) For a review of tomographic methods see:B.J. Pichler, J. Nucl. Med. 49 (2008) S5.
[8] (a) Y.N. Belokon, V.I. Bakhmutov, N.I. Chernoglazova, K.A. Kochetkov, S.V. Vitt, N.S. Garbalinskaya, V.M. Belikov, J. Chem. Soc., Perkin Trans. 1 (1988) 305;
(b) For reviews of methods of asymmetric preparation of α-methyl amino acids, see:C. Cativiela, M.D. Días-de-Villegas, Tetrahedron: Asymmetry 9 (1998) 3517;
(c) C. Cativiela, M.D. Días-de-Villegas, Tetrahedron: Asymmetry 11 (2000) 645;
(d) H. Vogt, S. Bräse, Org. Biomol. Chem. 5 (2007) 406;
(e) C. Najera, J.M. Sansano, Chem. Rev. 107 (2007) 4584;
(f) C. Cativiela, D. Días-de-Villegas, Tetrahedron: Asymmetry 18 (2007) 569.
[9] H. Franzen, L. Grehn, U.J. Ragnarsson, J. Chem. Soc., Chem. Commun. (1984) 1699.
[10] R. Jirásko, M. Holčapek, L. Kolářová, M. Nádvorník, A. Popkov, J. Mass Spectrom. 43 (2008) 1274.
[11] Bruker AXS Inc., SMART and SAINT, Area Detector Control and Integration Software, Madison, WI, USA, 2003.
[12] G.M. Sheldrick, SADABS, Program for Empirical Absorption Correction for Area Detectors, Version 2.10, University of Göttingen, Germany, 2003.
[13] Bruker, SHELXTL, Solution and Refinement Package, Version 6.12, Bruker AXS Inc., Madison, Wisconsin, USA, 2001.
[14] K. Brandenburg, DIAMOND, Crystal and Molecular Structure Vizualization, Version 3.1d, Crystal Impact GbR, Bonn, Germany, 2006.
[15] P. Řehulka, A. Popkov, M. Nádvorník, J. Planeta, K. Mazanec, J. Chmelík, J. Mass Spectrom. 41 (2006) 448.